Numerical study of multitime scaling in a solid system undergoing phase separation

Hiroshi Furukawa

Faculty of Education, Yamaguchi University, Yamaguchi 753, Japan
(Received 10 March 1989)

The multitime-scaling rule for time correlation functions is shown in systems undergoing phase separation. With the use of multitime scaling, the asymptotic form of the structural function, $\widetilde{S}(x) \propto x^4$, at small scaled wave numbers x is shown in a late state of phase separation in the diffusional system. A numerical simulation is performed to examine the multitime scaling. We use a discretized Cahn-Hilliard equation with the Oono-Puri free energy. The chemical potential is not conserved at all and may satisfy multitime scaling in the late stage of phase separation. Hence the suggested x^4 law of the structure function is justified.

I. INTRODUCTION

One of the central purposes for studying the dynamics of phase separation is to clarify pattern formation and its temporal evolution. Many studies have been devoted to this problem to show the validity of dynamical scaling in a late stage of phase separation. Dynamical scaling is usually represented for the structure function, $S_k(t)$:[1-3]

$$S_k(t) = \langle |\psi_\mathbf{k}(t)|^2 \rangle = R(t)^d \widetilde{S}(kR(t)) , \qquad (1.1)$$

where ψ is the order parameter, and k, t, and d are the wave number, time, and spatial dimension, respectively. Here $R(t)$ is a length scale, such as an average radius of clusters at time t. The growth rate of the ordered phase is characterized by the length scale $R(t)$, which depends on time algebraically:

$$R(t) \propto t^a , \qquad (1.2)$$

where a is a constant. The explicit form of the scaling function $\widetilde{S}$ depends on the spatial pattern of the order parameter. The sharp interface between two phases in the late stage of phase separation gives the tail of the form

$$\widetilde{S}(x) \propto x^{-(d+1)}, \quad x \gg 1 . \qquad (1.3)$$

When the order parameter is conserved, the scaling function $\widetilde{S}(x)$ should vanish at zero wave number $x = 0$, since $\psi_{\mathbf{k} \to 0}$ is a constant of the motion, whereas S_k at $k \neq 0$ becomes macroscopic [cf. (1.1)]. Thus one may expect

$$\widetilde{S}(x) \propto x^\delta, \quad \delta > 0 \qquad (1.4)$$

at small x. Then the structural function takes the maximum value at a finite wave number k_m. This wave number is proportional to the inverse length scale $k_m(t) \propto R^{-1}(t)$. The tail (1.3), called the Porod law,[4] reflects the interfacial effect and is valid only for large wave numbers.[5,6] For intermediate wave numbers near k_m the tail may be effectively approximated by a different exponent. If the bulk effect is important, then $\widetilde{S}(x)$ may have the tail x^{-2d}, which is only qualitative, however.[5]

The evaluation of the exponent δ is interesting. When the thermal fluctuation is effective we have $\delta = 2$. However, when the thermal fluctuation can be neglected the equality $\delta = 2$ loses its theoretical basis. Several experimental and numerical investigations[7-10] have suggested somehow an unexpected value of δ, i.e., $\delta \sim 4$, in the late stage of phase separation where no thermal fluctuation is effective. Recently, Yeung[9] tried to show an inequality $\delta \geq 4$ using the Cahn-Hilliard equation, which has no fluctuating force. The present author[11] pointed out that the following property (property 1) of the system is needed to obtain the inequality $\delta \geq 4$.

Property 1: The chemical potential $\mu(\mathbf{r}, t)$ is not a conserved quantity in the late stage of phase separation, and the local fluctuation of μ obeys the central-limit theorem. We have also shown that the exponent δ is really equal to 4, using property 1 together with property 2: *The time correlation function satisfies multitime scaling:*

$$\langle A_\mathbf{k}(t) B_{-\mathbf{k}}(t') \rangle = R(t)^{\alpha + d}$$
$$\times \widetilde{G}_{AB}(kR(t), R(t')/R(t)) , \qquad (1.5)$$

where α is a constant.

Although these two properties are quite reasonable, as discussed in a previous paper,[11] and therefore the resultant exponent $\delta = 4$ is plausible, no direct investigation of these properties has ever been shown. Furthermore, it is not certain if the numerical and experimental findings really indicate a true algebraic form $\widetilde{S}(x) \propto x^4$ or indicate only approximate functions. In fact, Tomita[12] showed that the numerical solution of the Langer, Bar-on, and Miller[13] type equation, which has no source for the x^4 term at small x, may exhibit an approximate x^4-like behavior at small x. This suggests that the direct experimental and numerical analyses of the structural function are not sufficient to examine such a behavior as x^4 at small x. The purpose of the present paper is to report the numerical study of the foregoing two properties. For the simulation we use the discretized Cahn-Hilliard equation with the Oono-Puri[14] free energy, which makes the numerical work efficient.

In Sec. II, we present a brief review of the multitime scaling and a subsequent derivation of the x^4 law for the structural function in the late stage of phase separation in a diffusional system. In Sec. III, the numerical model is

presented. This is a discretized Cahn-Hilliard model with the Oono-Puri free energy, and is equivalent to the Oono-Puri model. In Sec. IV, results of the numerical simulation are presented. Several properties of the chemical potential are presented, focusing on the multitime scaling of the zeroth Fourier component. These properties are sufficient to justify the x^4 law. Section V is devoted to conclusions and remarks.

II. MULTITIME SCALING AND DERIVATION OF $\delta = 4$

In this section we shall briefly review the previous discussions[11] for the multitime scaling and the subsequent derivation of $\delta = 4$. Let A and B be physical quantities as a function of position r and time t. The spatiotemporal correlation function between A and B is written as

$$G_{AB}(\mathbf{r},t,t') = \langle A(\mathbf{r},t)B(\mathbf{0},t') \rangle$$
$$- \langle A(\mathbf{r},t) \rangle \langle B(\mathbf{0},t') \rangle . \quad (2.1)$$

Here we assume that the system is spatially homogeneous. The scaling rule (1.5) is derived as follows. The time arguments t and t' can be characterized by the length scale $R(t)$ and $R(t')$ in the scaling regime. Therefore,

$$G_{AB}(\mathbf{r},t,t') = G'_{AB}(\mathbf{r},R(t),R(t')) . \quad (2.2)$$

Also, the simultaneous rescalings of three lengths, $r \to \lambda r$, $R(t) \to \lambda R(t)$, and $R(t') \to \lambda R(t')$, do not change the functional form of G_{AB}. Therefore,

$$G_{AB}(r,t,t') = \lambda^{-\alpha} \widetilde{G}_{AB}(\lambda r, \lambda R(t), \lambda R(t')) , \quad (2.3)$$

with α being a constant. By setting $\lambda R(t) = 1$ and Fourier transforming (2.3), we have the scaling rule (1.5). The single time scaling such as (1.1) is given by setting $t = t'$ in (1.5):

$$G_{AB,\mathbf{k}}(t,t) = \langle A_{\mathbf{k}}(t)B_{-\mathbf{k}}(t) \rangle$$
$$= R(t)^{d+\alpha} \widetilde{G}_{AB}(kR(t)) . \quad (2.4)$$

Equations (1.5) can also be rewritten as

$$G_{AB,\mathbf{k}}(t,t') = \langle A_{\mathbf{k}}(t)B_{-\mathbf{k}}(t) \rangle$$
$$\times U_{AB}(kR(t),R(t')/R(t)) , \quad (2.5)$$

where

$$U_{AB}(kR(t),1) = 1 . \quad (2.6)$$

Here we shall show $\delta = 4$ for the Cahn-Hilliard equation:

$$\frac{d}{dt}\psi(\mathbf{r},t) = -M\nabla^2\mu(\mathbf{r},t) ,$$
$$\frac{d}{dt}\psi_{\mathbf{k}}(t) = Mk^2\mu_{\mathbf{k}}(t) , \quad (2.7)$$

where M is the mobility and is assumed to be time independent, and μ is the chemical potential. From (2.7) the equation of motion for the structural function $S_k(t)$ is

readily given as

$$\frac{d}{dt}S_{\mathbf{k}}(t) = 2(Mk^2)^2 \int_0^t \langle \mu_{\mathbf{k}}(t)\mu_{-\mathbf{k}}(t') \rangle dt' . \quad (2.8)$$

Here we have assumed that $\psi(\mathbf{r},t)$ is real and that in the scaling regime

$$|\langle \mu_{\mathbf{k}}(t)\psi_{-\mathbf{k}}(t) \rangle| \gg |\langle \mu_{\mathbf{k}}(t)\psi_{-\mathbf{k}}(0) \rangle| .$$

The correlation function $\langle \mu_{\mathbf{k}}(t)\mu_{-\mathbf{k}}(t') \rangle$ is scaled as

$$\langle \mu_{\mathbf{k}}(t)\mu_{-\mathbf{k}}(t') \rangle = R(t)^{-\phi}\widetilde{G}_{\mu\mu}(kR(t))$$
$$\times U_{\mu\mu}(kR(t),R(t')/R(t)) , \quad (2.9)$$

with

$$U_{\mu\mu}(kR(t),1) = 1 . \quad (2.10)$$

Here $\phi = 2 - d$, since $\mu(\mathbf{r}) \propto 1/R$ in the scaling regime. Since the chemical potential is not a conserved quantity in the nonequilibrium state,

$$\lim_{k \to 0} \langle |\mu_{\mathbf{k}}(t)|^2 \rangle$$

does not vanish. Therefore, the correlation function (2.10) takes the form for small k

$$\lim_{k \to 0} \langle \mu_{\mathbf{k}}(t)\mu_{-\mathbf{k}}(t') \rangle \propto R(t)^{d-2}\mathcal{U}_{\mu\mu}(t'/t) ,$$
$$\mathcal{U}_{\mu\mu}(1) = 1 . \quad (2.11)$$

Here

$$\mathcal{U}_{\mu\mu}(t'/t) = U_{\mu\mu}(0,R(t')/R(t)) ,$$

and we have used (1.2). From (2.8) and (2.11) we obtain for small k

$$\frac{d}{dt}S_k(t) \propto 2(Mk^2)^2R(t)^{d-2}ct , \quad k \sim 0 , \quad (2.12)$$

where $c = \int_0^1 \mathcal{U}_{\mu\mu}(x)dx$. In a relaxational system, no oscillatory decay of $\mathcal{U}$ in time can be expected. Thus $\mathcal{U}(x)$ would be a monotonic function, and therefore c should be positive. From (2.12) we find $\delta = 4$.

Before closing this section, it is interesting to examine the effect of the thermal fluctuation on the asymptotic behavior of the structural function. From (2.7) we observe

$$S_k(t) \sim 2Mk^2\langle \mu_{\mathbf{k}}(t)\psi_{-\mathbf{k}}(t) \rangle t$$

at small k. When there is no thermal fluctuation as we discussed here, the driving force is the surface tension and the quantity $\langle \mu_{\mathbf{k}}(t)\psi_{-\mathbf{k}}(t) \rangle$, which has the dimension of energy, is of the order $(kR)^2\sigma R^{d-1}$ at small kR. Here σ is the surface tension and is of the order $k_B T_c \xi^{1-d}$, where k_B is the Boltzmann constant, T_c is the critical temperature of the phase separation, and ξ is a microscopic length scale associated with the thermal fluctuation such as the thermal correlation length in one phase. When the thermal fluctuation is effective, $\langle \mu_{\mathbf{k}}\psi_{-\mathbf{k}} \rangle$ is of the order of thermal energy $k_B T$. Strictly speaking, $k_B T$ comes from the fluctuation-dissipation relation.[1] Then we have another asymptotic behavior $\widetilde{S}(x) \sim x^2$. The crossover from one to the other occurs at

$(kR)^2 \sigma R^{d-1} \sim k_B T$, i.e., at

$$k^2 R(t)^2 = x_c(t)^2 \sim \frac{T}{T_c} \left[\frac{\xi}{R(t)} \right]^{d-1} .$$

Namely, we may find $\widetilde{S}(x) \sim x^2$ for $x < x_c$, whereas we may find $\widetilde{S}(x) \sim x^4$ for $x > x_c$, where $x \equiv kR$. Hereafter we do not take the effect of the thermal fluctuation into consideration, i.e., we consider only the case of large $R(t)$.

III. NUMERICAL MODEL

To solve numerically the Cahn-Hilliard equation (2.7), this equation is discretized as[14-16]

$$\psi(t+\tau, n) - \psi(t, n) = -\tau \mathcal{L} \mathcal{H}(\{\psi\}) . \tag{3.1}$$

Here n indicates a lattice site n in the discrete space, τ indicates a discrete time interval, and $\mathcal{L}$ is the discrete Laplacian. The quantity $\mathcal{H}$ is proportional to μ: $\mathcal{H} = M\mu$. Hereafter we set $M = 1$ and thus we do not distinguish $\mathcal{H}$ from μ. The chemical potential in the discrete space is written as

$$\mu = \mu_0(\{\psi\}) + g\mathcal{L}\psi(t, n) , \tag{3.2}$$

where g is a constant representing the strength of the interaction. Usually the noninteracting part of the scaled chemical potential, μ_0, takes the form

$$\mu_0 = \psi - \psi^3 , \tag{3.3}$$

where we have omitted a trivial proportionality constant on the right-hand side of (3.3). Oono and Puri[14] introduced another type of chemical potential:

$$\mu_0 = A \tanh(\psi) - \psi . \tag{3.4}$$

With the chemical potential (3.4) we can use a very large time interval $\tau \sim 1$ without any undesirable instabilities due to the discretization.[14] Therefore, if we employ (3.4), then we can treat (3.1) as essentially a discrete model different from the original continuum model (2.7). Thus, the numerical computation becomes efficient. It is expected that there is no essential difference between the continuum model and the discrete model in the scaling regime where the characteristic length and time scales are much longer than those of model equations and any meaningful changes in space and time are regarded as continuous.

Let us consider instabilities in the preceding discretized model.[16] We may define the discrete Laplacian $\mathcal{L}$ as

$$\Delta r^2 \mathcal{L} F(t, n) = \frac{1}{z} \sum_{NN} (F_{NN}) - F , \tag{3.5}$$

where F_{NN} is F in the nearest-neighbor sites and Δr is the lattice constant and z is the number of nearest-neighbor cells ($z = 4$ and 6 for the square lattice and the simple-cubic lattice, respectively). Linearizing and Fourier analyzing (3.1), we have a transformation equation

$$\delta \psi_k(t+\tau) = H_k \delta \psi_k(t) .$$

The system becomes unstable when $|H_k| > 1$ for any

value of the wave number k. The instability $H_k > 1$ corresponds to the spinodal decomposition, while the instability $H_k < -1$ has no counterpart in the continuous equation. This seems to suggest that we must choose $H_k > -1$ for all values of k. The former instability occurs at small wave numbers, whereas the latter occurs at large wave numbers. To avoid the latter instability for all wave numbers we may set

$$H_k > -1 \quad \text{at} \quad k_x, k_y, k_z = \frac{\pi}{\Delta r} .$$

This is because the first instability occurs at the largest wave number ($\pi/\Delta r, \pi/\Delta r, \pi/\Delta r$).[16] In this sense the latter instability gives rise to an antiferromagnetic-like pattern. The foregoing condition gives, for the chemical potential (3.3),

$$(2g - \Delta r^2)\tau < \Delta r^4 , \tag{3.6}$$

and for (3.4),

$$[2g - (A-1)\Delta r^2]\tau < \Delta r^4 . \tag{3.7}$$

We use the following values of parameters throughout the present work:

$$g = \tfrac{1}{4}, \quad \Delta r = 1, \quad A = 1.3 . \tag{3.8}$$

Then for the square lattice, (3.6) and (3.7) become $\tau > -2$ and $\tau < 5$, respectively. Thus, with $\tau = 1$ no antiferromagnetic-like instability is expected to occur for either (3.3) or (3.4). Actually, however, an antiferromagnetic-like instability is observed for (3.3), whereas it is not observed for (3.4) (see Fig. 1). The essential difference between (3.3) and (3.4) seems to be the difference between asymptotic forms of μ_0 at large values of the order parameter. Oono and Puri[14] explained the equation (3.1) with $\tau = 1$ as a nonlinear mapping equation for $\psi(t)$. With (3.4) this mapping gives a rather smooth approach of ψ to its nonzero fixed points $\pm\psi_{\text{fix}}$, whereas with (3.3) the approach is oscillatory. If we use $\mu_0 = \epsilon\psi - \psi^3$ instead of (3.3), then such an oscillation can be removed for a small positive value of ϵ, and no antiferromagnetic-like instability occurs even for a finite $\tau (= 1)$.[17] The Oono-Puri model [$\tau = 1$ and (3.4) for μ_0] is essentially a discrete model, but it must give results essentially equivalent to those by the continuum model in the late stage of phase separation.[18]

IV. RESULTS

We studied numerically the discretized equation (3.1) with $\tau = 1$ and with (3.4) for μ_0 with a periodic boundary condition. Throughout the present study we used the values of parameters (3.8). The parameter $A = 1.3$ gives the fixed points $\psi_{\text{fix}} \sim \pm 1$. Oono and Puri[14] used $g = \tfrac{1}{2}$ and $A = 1.3$, for which, however, we encountered an antiferromagnetic-like instability and a subsequent divergence in numerical computation. Such a divergence can be removed if we use a spherical discrete Laplacian on the square lattice:[14]

$$\mathcal{L}F(t, n) = \tfrac{1}{6} \sum_{NN} (F_{NN}) + \tfrac{1}{12} \sum_{NNN} (F_{NNN}) - F , \tag{4.1}$$
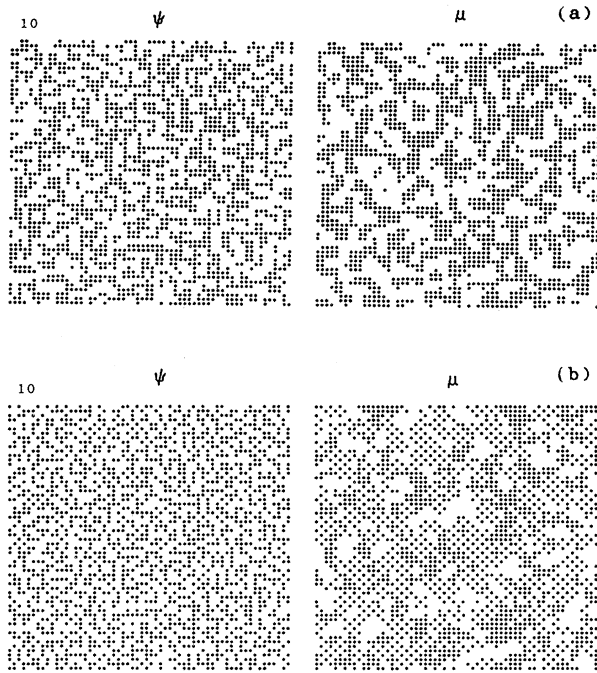
FIG. 1. Spatial patterns of the order parameter ψ (left) and the chemical potential μ (right) at time 10 ($\tau = 1$) on the square lattice, generated by (3.1). Asterisks indicate lattice sites with $\psi > 0$ or $\mu < 0$. (a) Case of (3.4) with the discrete Laplacian (3.5) and parameters (3.8). No antiferromagnetic-like pattern is seen. (b) Case of (3.3) with (3.5). In this case the antiferromagnetic-like patterns are seen clearly for the chemical potential. Shortly after, the numerical computation encountered the divergence.

FIG. 2. Early time (upper: $t = 40$) and late time (lower: $t = 3000$) spatial patterns of the order parameter (left) and the chemical potential (right) for the discrete model ($\tau = 1$) with (3.4) and (4.1) (Oono-Puri model). We used parameters (3.8) throughout this work.

where F_{NNN} is F in the next-nearest-neighbor sites. In two dimensions we have used the spherical discrete Laplacian (4.1). But we have found no essential difference between (4.1) and (3.5) with the values of parameters (3.8). In three dimensions we have used the discrete Laplacian (3.5), only.

One reason to use a value of g such as (3.8) is that our three-dimensional system ($30 \times 30 \times 30$) is not so large. The system size is effectively larger for a smaller value of g. The simulation was done in two and three dimensions (on the square and the simple-cubic lattice) for the time interval $0 \leq t \leq 3000\tau$ ($\tau = 1$).

Quenches are done at the center of the miscibility gap:

$$\langle \psi \rangle = 0 . \tag{4.2}$$

Initial values of the order parameter on lattice sites are randomly set between $-0.25 \sim 0.25$. In Fig. 2 we show two-dimensional spatial patterns of the order parameter and the chemical potential on a square lattice in early and late stages of phase separation. The system size is 60×60. Asterisks indicate lattice sites with $\psi > 0$ or $\mu < 0$ in each figure. In the early stage of phase separation, the pattern of the order parameter resembles that of the chemical potential. This indicates that the chemical potential may be approximately proportional to the order
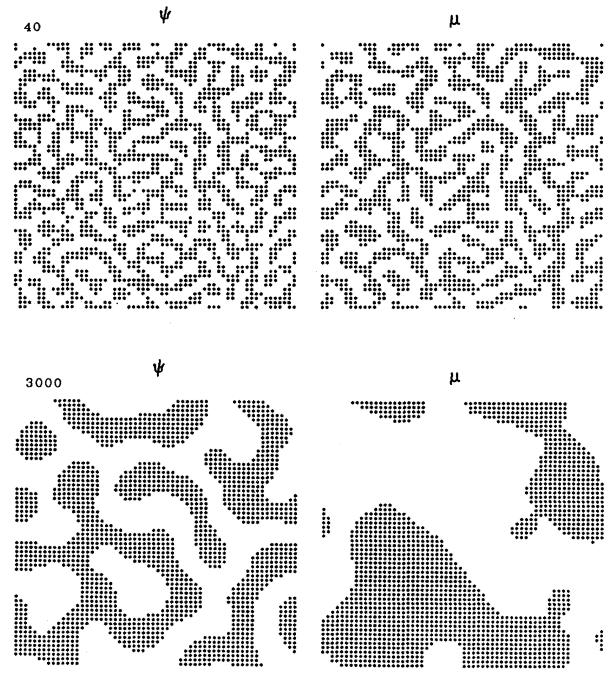
parameter, and therefore the Cahn-Hilliard linearized theory may be valid in the initial stage. In the late stage the spatial pattern of the chemical potential is not the same as that of the order parameter. This suggests that the chemical potential is not a conserved quantity. This can be more clearly seen in Fig. 3. Here we plot the following quantities (zeroth Fourier components) on the simple-cubic lattice:

$$N^{-1/2} \sum_{n=1}^{N} \psi(n,t), \quad N^{-1/2} \sum_{n=1}^{N} \mu(n,t) ,$$

where N is the number of sites.

We examined the Fourier transformation of the same time correlation function, $\langle |\mu_k(t)^2| \rangle$. This quantity is scaled as [cf. (2.4)]

$$\langle |\mu_k(t)^2| \rangle \propto R(t)^{-\phi} \tilde{G}_{\mu\mu}(kR(t)) , \tag{4.3}$$

where $\phi = 2 - d$. The wave number k means the spherically averaged one.[19] In Fig. 4, $\langle |\mu_k(t)|^2 \rangle$ at $k = 0$ in two and three dimensions are plotted as functions of time in log-log scale. Although these quantities are very fluctuating, the simulation is consistent with

$$\langle |\mu_0(t)|^2 \rangle \propto R(t)^{-\phi}, \quad \phi = 2 - d \tag{4.4}$$
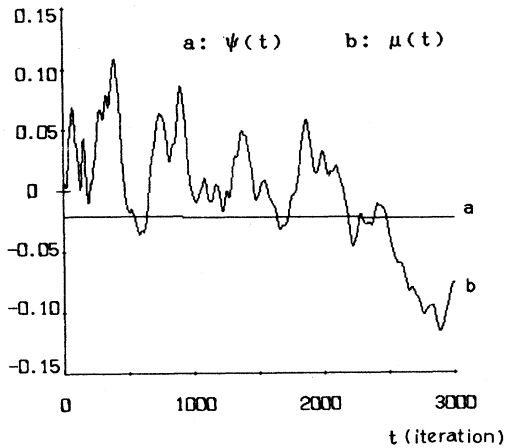
and

$$R(t) \propto t^{1/3} . \tag{4.5}$$

FIG. 3. Temporal evolutions of zeroth Fourier components of the order parameter ψ and the chemical potential μ for the three-dimensional Oono-Puri model with (3.4) and (3.5).
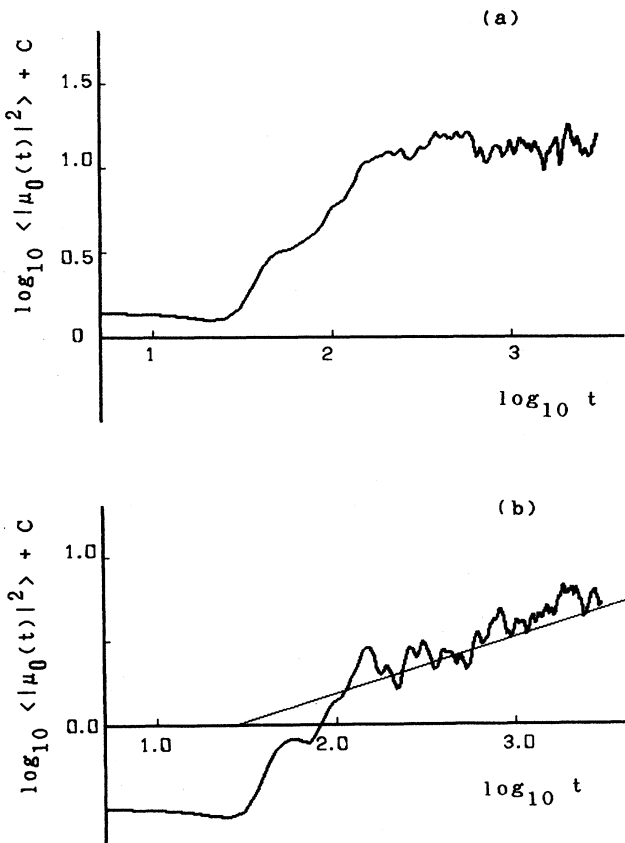
Figure 5 shows three-dimensional scaling functions $\tilde{G}_{\mu\mu}$ and $\tilde{S}$ ($=\tilde{G}_{\psi\psi}$) in log-log scale (the system size in this case is $20\times20\times20$). Here we employed (4.5) and calculated the scaling function simply by

$$\tilde{G}_{\mu\mu}(x)=R^{\phi}\langle|\mu_k(t)|^2\rangle$$

with $x=kR(t)$. The shapes of the two scaling functions are quite different from each other at small wave numbers. This is because the chemical potential is not conserved, whereas the order parameter is conserved.

We also calculated the normalized autocorrelation function of the zeroth Fourier component of the chemical potential, i.e.,

$$\mathcal{U}'_{\mu\mu}(t,t')=\frac{\langle\mu_k(t)\mu_{-k}(t')\rangle}{\langle|\mu_k(t)|^2\rangle}\bigg|_{k=0},\quad t\geq t'. \quad (4.6)$$

To examine the scaling property of (4.6) we divided the region of time t into six subregions:

$$500(p-1)<t\leq500p,\quad p=1,2,\ldots,6$$

and we averaged (4.6) for a given value of t'/t (≤1) in each subregion to get $\mathcal{U}_{\mu\mu}(t'/t,p)$. Here $t_0<t'\leq t$, where $t_0\sim50$. $\mathcal{U}_{\mu\mu}(t'/t,p)$ indicates the average decay of the correlation from each time subregion as a function of t'.

FIG. 4. $\langle|\mu_k(t)|^2\rangle$ at $k=0$ as functions of t. (a) Two-dimensional case. Data are averaged over 37 runs on the square lattice of size 60×60. (b) Three-dimensional case. Data are averaged over 32 runs on the simple-cubic lattice of size $30\times30\times30$. The straight line indicates the slope $\frac{1}{3}$.
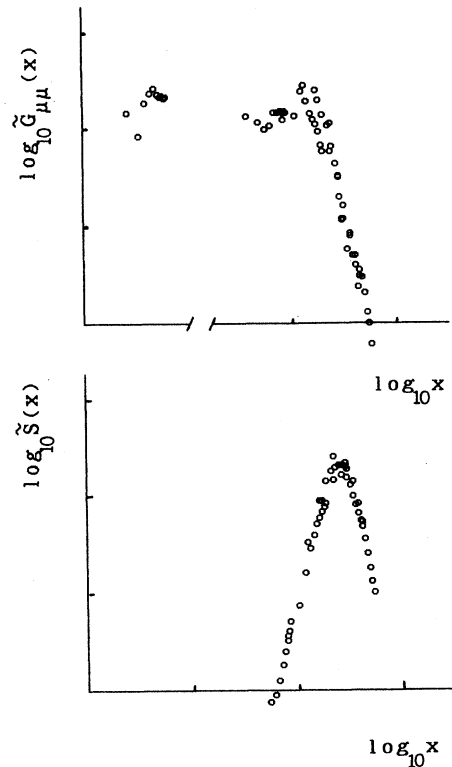
FIG. 5. Three-dimensional scaling functions $\tilde{G}_{\mu\mu}(x)$ (upper) and $\tilde{S}(x)$ (lower) in log-log scale. The scaling unit is arbitrary, but the vertical and horizontal units are the same. The data are averaged over 29 runs on the simple-cubic lattice of size $20\times20\times20$.
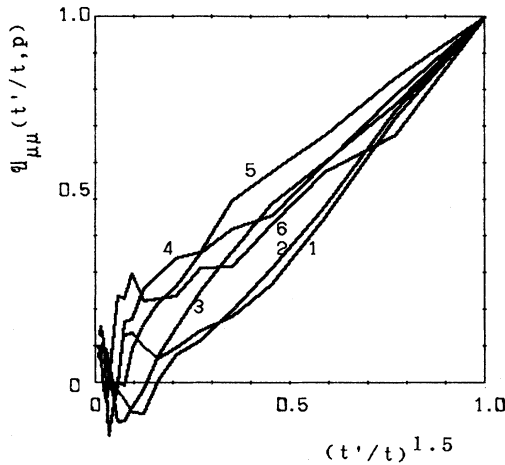
FIG. 6. Three-dimensional autocorrelation function (4.6) averaged in time subregions $500(p-1) < t \leq 500p$ $(p = 1,2, \ldots ,6)$. Here numbers on the figure indicate p. The same data as for Fig. 4(b) are used.

In Fig. 6 these quantities in three dimensions are shown as functions of $(t'/t)^{1.5}$. If the decay of the autocorrelation function is, for instance, a modified exponential function

$$\exp(-\gamma t'^{1.5}) ,$$

then the scaling $t' \rightarrow t'/p$ gives the scaling of the damping coefficient, $\gamma \rightarrow p^{1.5}\gamma$, and therefore, the slope of $\mathcal{U}_{\mu\mu}(t'/t,p)$ for $p = 6$ may be $6^{1.5} = 14.7$ times larger than that for $p = 1$. However, Fig. 6 shows a different phenomenon. That is, the autocorrelation function $\mathcal{U}_{\mu\mu}(t'/t,p)$ is rather independent of p:
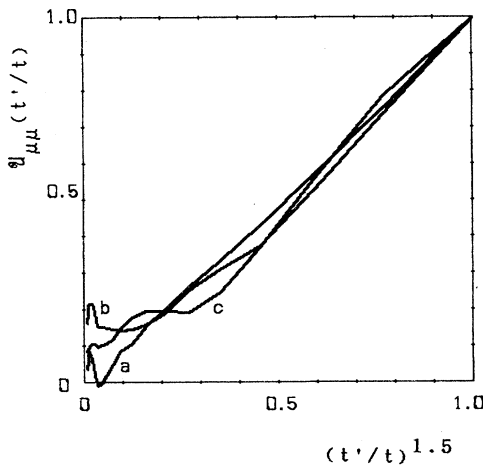

FIG. 7. Three-dimensional scaling autocorrelation functions $\mathcal{U}_{\mu\mu}(t'/t)$ on simple-cubic lattices. a: The system size is $30 \times 30 \times 30$, and the same data for Fig. 6 and Fig. 4(b) are used. b: The system size is $20 \times 20 \times 20$, and data are averaged over 30 runs. c: The system size is $15 \times 15 \times 15$, and data are averaged over 15 runs.

$$\mathcal{U}_{\mu\mu}(t'/t,p) = \mathcal{U}_{\mu\mu}(t'/t) . \tag{4.7}$$

The multitime-scaling function $\mathcal{U}_{\mu\mu}(t'/t)$ [see also (2.11)] is calculated in the same way as $\mathcal{U}_{\mu\mu}(t'/t,p)$ for the whole time interval $t_0 \leq t \leq 3000$. In Fig. 7, scaling functions for different system sizes in three dimensions are shown. We find that the system size effect is not important. The scaling autocorrelation function $\mathcal{U}_{\mu\mu}(x)$ in three dimensions exhibits a simple algebraic decay

$$\mathcal{U}_{\mu\mu}(x) \sim x^{-1.5}, \quad x \leq 1 . \tag{4.8}$$

However, in two dimensions we could not find such a simple decay law (Fig. 8).

V. CONCLUSIONS AND REMARKS

The purpose of the present study was to clarify statistical properties of the chemical potential in the system un-
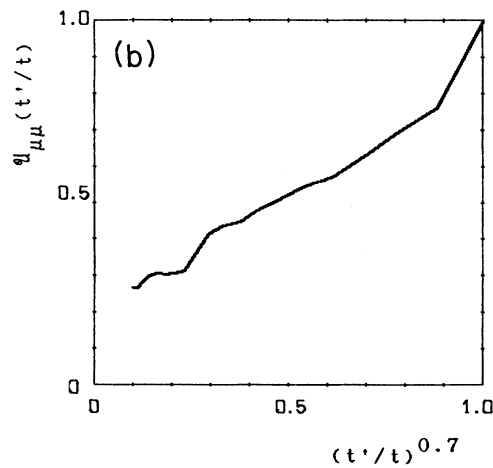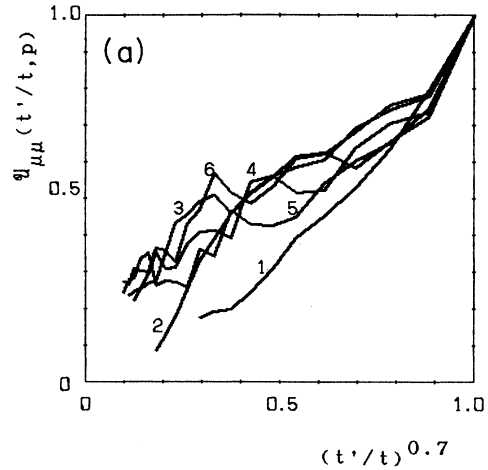

FIG. 8. Two-dimensional scaling autocorrelation function on the square lattice of size 60×60. The same data for Fig. 4(a) are used. (a) Autocorrelation function (4.6) averaged in time subregions $300(p-1) < t \leq 500p$ $(p = 1,2, \ldots ,6)$. Here numbers on figure indicate p. (b) Corresponding scaling autocorrelation function.

dergoing phase separation. In the later stage of phase separation the chemical potential is not a conserved quantity at all. We found that the multitime scaling may hold for the fluctuation of the chemical potential. The multitime scaling is a natural extension of a single time scaling such as (1.1). Statistical properties of the chemical potential studied here are sufficient to justify the asymptotic behavior of the structural function, $\widetilde{S}(x) \propto x^4$ at small x. The study of the multitime scaling at finite wave numbers for the chemical potential and also for other quantities is left as a future problem.

The order parameter depends on the values of the chemical potential at earlier times. Thus the chemical potential may approach the scaling behavior faster than the order parameter. However, it should be noted that the fluctuation is larger in the chemical potential than in the order parameter. Therefore, it is not always easier to examine the scaling behavior by the chemical potential than by the order parameter.

So far all quenches are done at the center of the miscibility gap. This would not lose the generality of present conclusions. For a quench near the coexistence curve the cluster shape is rather spherical, whereas it is interconnected near the center of the miscibility gap. However, the statistical nature of the fluctuation of the chemical potential would be the same. That is, the fluctuation of the chemical potential is nonconservative and obeys the central-limit theorem. In fact, we have numerically ascertained these properties of the chemical potential for the quench near the coexistence curve. Due to the small system size and the elongation of the time scale of the fluctuation, we could not examine the multitime scaling of the chemical potential for the quench near the coexistence curve.

We have considered a model for a solid system. Essentially the same conclusion is expected for the viscous fluid. This is because we expect that the cluster mobility may have a nonvanishing zeroth Fourier component $M_0(t)$ also for the fluid, that the driving force corresponding to the chemical potential may be nonconservative, and that the order parameter would obey a generalized diffusion equation like the Cahn-Hilliard equation. These three are the main factors for all conclusions obtained in this work.

[1]H. Furukawa, Adv. Phys. **34**, 703 (1985).

[2]K. Binder, in *Statistical Physics,* edited by H. E. Stanley (North-Holland, Amsterdam, 1986).

[3]J. D. Gunton, M. San Miguel, and P. S. Sahni, in *Phase Transitions and Critical Phenomena,* edited by C. Domb and J. L. Lebowitz (Academic, New York, 1983).

[4]G. Pord, in *Small Angle X-Ray Scattering,* edited by O. Glatter and L. Kratky (Academic, New York, 1883).

[5]H. Furukawa, Phys. Rev. A **23**, 1535 (1981).

[6]H. Tomita, Prog. Theor. Phys. **72**, 656 (1984).

[7]S. Spooner, in *Kinetics of Aggregation and Gelation,* edited by F. Family and D. P. Landau (North-Holland, Amsterdam, 1984).

[8]J. K. Hoffer and D. N. Sinha, Phys. Rev. A **33**, 1918 (1986).

[9]C. Yeung, Phys. Rev. Lett. **61**, 1135 (1988).

[10]P. Fratzl and J. L. Lebowitz (unpublished). Other experimental data also seem to suggest $\delta = 4$, though authors did not point it out explicitly. See, for instance, S. Katano and M. Iizumi, Phys. Rev. Lett. **52**, 835 (1984); P. Wiltzius, F. S. Bates, and W. R. Heffner, *ibid.* **60**, 1538 (1988); T. Hashimoto, M. Takenaka, and T. Izumitani (unpublished).

[11]H. Furukawa, J. Phys. Soc. Jpn. **58**, 216 (1989).

[12]H. Tomita (unpublished).

[13]J. S. Langer, M. Bar-on, and H. P. Miller, Phys. Rev. A **11**, 1414 (1975); H. Tomita, Prog. Theor. Phys. **59**, 1116 (1978); G. F. Mazenko and M. Zannetti, Phys. Rev. Lett. **53**, 2106 (1984).

[14]Y. Oono and S. Puri, Phys. Rev. Lett. **58**, 386 (1987); Phys. Rev. A **38**, 434 (1988); **38**, 1542 (1988).

[15]R. Toral, A. Chakrabarti, and J. D. Gunton, Phys. Rev. Lett. **60**, 2311 (1988); O. T. Valls and G. F. Mazenko, Phys. Rev. B **34**, 7941 (1986); A. Milchev, K. Binder, and D. W. Heermann, Z. Phys. B **63**, 521 (1986); R. Petschek and H. Metiu, J. Chem. Phys. **79**, 3443 (1985).

[16]T. M. Rogers, K. R. Elder, and Rashmi C. Desai, Phys. Rev. B **37**, 9638 (1988).

[17]In this case the model is a suitable discrete model, giving essentially the equivalent result by the discrete model with (3.4). Notice that the constant ϵ cannot be scaled out in the discrete model. This is the peculiarity of the discrete model.

[18]J. D. Gunton, E. T. Gawlinski, A. Chakrabarti, and K. Kaski, J. Appl. Crystallogr. **21**, 811 (1988).

[19]The original wave number in a lattice space is such that $\mathbf{k} = (2\pi/L)(\pm m_x, \pm m_y, \pm m_z)$ $(m = 0, 1, 2, 3, \dots)$ and L is the linear dimension of the system $(L = N^{1/3})$.